ADAM17-Dependent c-MET-STAT3 Signaling Mediates Resistance to MEK Inhibitors in KRAS Mutant Colorectal Cancer

Van Schaeybroeck, S., Kalimutho, M., Dunne, P. D., Carson, R., Allen, W., Jithesh, P. V., Redmond, K. L., Sasazuki, T., Shirasawa, S., Blayney, J., Michieli, P., Fenning, C., Lenz, H-J., Lawler, M., Longley, D. B., & Johnston, P. G. (2014). ADAM17-Dependent c-MET-STAT3 Signaling Mediates Resistance to MEK Inhibitors in *KRAS* Mutant Colorectal Cancer. *Cell Reports*, *7*(6), 1940-1955. https://doi.org/10.1016/j.celrep.2014.05.032

Published in:
Cell Reports

Document Version:
Publisher's PDF, also known as Version of record

Queen's University Belfast - Research Portal:
Link to publication record in Queen's University Belfast Research Portal

Publisher rights
© 2014 The Authors
This is an open access article under the CC BY-NC-ND license (http://creativecommons.org/licenses/by-nc-nd/3.0/)which permits distribution and reproduction for non-commercial purposes, provided the author and source are cited.

General rights
Copyright for the publications made accessible via the Queen's University Belfast Research Portal is retained by the author(s) and / or other copyright owners and it is a condition of accessing these publications that users recognise and abide by the legal requirements associated with these rights.

Take down policy
The Research Portal is Queen's institutional repository that provides access to Queen's research output. Every effort has been made to ensure that content in the Research Portal does not infringe any person's rights, or applicable UK laws. If you discover content in the Research Portal that you believe breaches copyright or violates any law, please contact openaccess@qub.ac.uk.

Download date:08. May. 2023

OPEN ACCESS
CellPress

Cell Reports
Article

ADAM17-Dependent c-MET-STAT3 Signaling Mediates Resistance to MEK Inhibitors in *KRAS* Mutant Colorectal Cancer

Sandra Van Schaeybroeck,[1,7] Murugan Kalimutho,[1,7] Philip D. Dunne,[1] Robbie Carson,[1] Wendy Allen,[1] Puthen V. Jithesh,[1] Keara L. Redmond,[1] Takehiko Sasazuki,[2] Senji Shirasawa,[3] Jaine Blayney,[1] Paolo Michieli,[4,5] Cathy Fenning,[1] Heinz-Josef Lenz,[6] Mark Lawler,[1] Daniel B. Longley,[1] and Patrick G. Johnston[1,*]

[1]Centre for Cancer Research and Cell Biology, School of Medicine, Dentistry and Biomedical Science, Queen's University Belfast, 97 Lisburn Road, Belfast BT9 7AE, UK
[2]Institute for Advanced Study, Kyushu University, Higashi-ku, Fukuoka 812-8582, Japan
[3]Department of Cell Biology, Faculty of Medicine, Fukuoka University, Jonan-Ku, Fukuoka 814-0180, Japan
[4]Laboratory of Experimental Therapy, Candiolo Cancer Institute–FPO, IRCCS, Candiolo, Torino 10060, Italy
[5]Department of Oncology, University of Torino Medical School, Candiolo, Torino 10060, Italy
[6]Division of Medical Oncology, University of Southern California/Norris Comprehensive Cancer Center, Keck School of Medicine, Los Angeles, CA 90033, USA
[7]Co-first author
*Correspondence: p.johnston@qub.ac.uk
http://dx.doi.org/10.1016/j.celrep.2014.05.032
This is an open access article under the CC BY-NC-ND license (http://creativecommons.org/licenses/by-nc-nd/3.0/).

SUMMARY

There are currently no approved targeted therapies for advanced *KRAS* mutant (*KRAS*MT) colorectal cancer (CRC). Using a unique systems biology approach, we identified JAK1/2-dependent activation of STAT3 as the key mediator of resistance to MEK inhibitors in *KRAS*MT CRC in vitro and in vivo. Further analyses identified acute increases in c-MET activity following treatment with MEK inhibitors in *KRAS*MT CRC models, which was demonstrated to promote JAK1/2-STAT3-mediated resistance. Furthermore, activation of c-MET following MEK inhibition was found to be due to inhibition of the ERK-dependent metalloprotease ADAM17, which normally inhibits c-MET signaling by promoting shedding of its endogenous antagonist, soluble "decoy" MET. Most importantly, pharmacological blockade of this resistance pathway with either c-MET or JAK1/2 inhibitors synergistically increased MEK-inhibitor-induced apoptosis and growth inhibition in vitro and in vivo in *KRAS*MT models, providing clear rationales for the clinical assessment of these combinations in *KRAS*MT CRC patients.

INTRODUCTION

Oncogenic activating mutations in *KRAS* occur in 40%–45% of patients with colorectal cancer (CRC) (Maughan et al., 2011). Oncogenic point mutations in *KRAS* occur mainly in codons 12 or 13, which alter its guanine nucleotide-binding site, resulting in constitutive activation of GTP-bound Ras and aberrant downstream signaling (Clark et al., 1985). *KRAS* mutant (*KRAS*MT) CRC is resistant to epidermal growth factor receptor (EGFR)-targeted therapies (Van Cutsem et al., 2011); therefore, identification of novel therapies for *KRAS*MT CRC is urgently needed to address a currently unmet clinical need.

Therapeutic targeting of Ras downstream effectors, such as the Raf kinase and MEK1/2, has shown limited activity in *KRAS*MT CRC. Rational combination studies of MEK inhibition (MEKi) with therapeutic strategies to block compensatory signaling mechanisms are urgently needed to increase the response and survival of these patients. A number of chemical compound screens using isogenic *KRAS* wild-type (*KRAS*WT) and *KRAS*MT cell lines have identified compounds that exhibit greater lethality in tumor cells harboring mutations in *KRAS* (Torrance et al., 2001). However, translation of these studies into the clinical setting has been impeded by the difficulty of identifying the protein target for these compounds, which is a prerequisite for further drug development. More recently, genome-wide small hairpin RNA (shRNA) screens have been employed to unravel novel biological aspects associated with oncogenic *KRAS* (Barbie et al., 2009; Luo et al., 2009; Scholl et al., 2009).

In this study, we used a unique systems biology approach that incorporates gene-expression data from MEKi-treated *KRAS*WT and *KRAS*MT preclinical CRC models, primary colorectal tumors, preclinical and clinical chemoresistant models, and in silico *KRAS* gene signatures to identify pathways that are essential for the survival of *KRAS*MT CRC in the context of MEKi or chemotherapy treatment. We identified a druggable mechanism of resistance to MEK inhibitors in *KRAS*MT CRC mediated by c-MET via JAK1/2-STAT3 that is acutely induced as a consequence of suppression of MEK-dependent, ADAM17-mediated shedding of the soluble decoy MET receptor. In addition, we identified the JAK/STAT3 pathway as a mediator of resistance to standard chemotherapy in *KRAS*MT CRC.

RESULTS

Generation of Oncogenic *KRAS* Transcriptomic Signatures

In order to identify novel pathways associated with constitutively active KRAS and novel therapeutic strategies for *KRAS*MT CRC, we performed transcriptional profiling of *KRAS*MT and *KRAS*WT primary CRC tumors and isogenic *KRAS*MT and *KRAS*WT CRC xenograft models that were treated or untreated with the MEK inhibitor AZD6244 (Van Schaeybroeck et al., 2011). Microarray analysis revealed that 314 genes were constitutively altered between HCT116 (G13D) *KRAS*MT and HKH-2 *KRAS*WT xenografts (2-fold difference and $p < 0.001$; Table S1), and 304 genes were altered following treatment with AZD6244 in the HCT116 *KRAS*MT xenograft model (2-fold difference and $p < 0.01$; Table S2). In the analyses of the clinical samples, 443 genes were altered between *KRAS*MT and *KRAS*WT CRC patients following normalization and filtering (1.5-fold and $p < 0.05$; Table S3).

Pathway Analyses

To identify pathways that are both required for survival of *KRAS*MT CRC *and* involved in resistance to MEKi, we carried out pathway analyses using the top 300 transcripts for *KRAS*MT and *KRAS*WT in in vivo gene lists, clinical gene lists, and publicly available *KRAS* signatures (Chang et al., 2009; Figure S1A). In each case, we selected the top 35 pathways that were altered between sample groups (Figure S1B). A comparison of the pathway analysis results showed that ERK1/2 signaling, c-MET signaling, insulin growth factor (IGF) signaling, JAK/STAT signaling, regulation of the epithelial-mesenchymal transition (EMT), chemokines, PLAU signaling, and BAD were altered in more than three out of four data sets in the gene lists representing both oncogenic *KRAS* and MEKi resistance. As combinations of 5-FU/oxaliplatin or 5-FU/irinotecan remain the cornerstone of treatment for advanced CRC patients, we also carried out pathway analyses using the top 300 transcripts derived from our recently published chemotherapy-resistance in vitro and clinical gene lists (Allen et al., 2012; Stevenson et al., 2012; Figure S1C). A comparison of all these pathway analyses revealed that JAK/STAT and Oncostatin signaling, regulation of EMT, platelet-derived growth factor receptor (PDGFR) signaling, interferon signaling, and Metaphase checkpoint were altered in more than four out of five data sets in the gene lists representing both oncogenic *KRAS* and chemotherapy resistance.

To identify key functional genes/targets for *KRAS*MT CRC and sensitizers to MEKi and/or chemotherapy treatment in *KRAS*MT CRC, we used an RNAi screening approach targeting proteins that lie at nodal points in the top 35 pathways (Figure S1A). The effect of downregulating each of these proteins on cell viability was tested in *KRAS*MT and WT HCT116 isogenic models. The effect of RNAi against the positive hits from the primary KRAS synthetic lethal screen was further tested in the absence and presence of MEKi (AZD6244) or 5-FU (Figure S1A).

JAK1/2-STAT3: A Key Regulator of Viability and Response to MEKi and 5-FU in *KRAS*MT CRC Cells

The *KRAS*MT HCT116 and *KRAS*WT HKH-2 isogenic paired cell line model was used (Shirasawa et al., 1993) and single small interfering RNAs (siRNAs) against 160 targets were assessed in the primary screen. RNAi against KRAS resulted in a significant reduction in cell viability in the HCT116 cell line, but not in HKH-2 cells, confirming the KRAS dependency of the HCT116 cells (Figure S1D). siRNAs targeting 77 mRNAs were found to more significantly affect the viability of *KRAS*MT HCT116 cells compared with a *KRAS*WT daughter cell line (Figure S1D). Moreover, 21 of these 77 siRNAs also enhanced sensitivity to MEKi treatment in the *KRAS*MT cell line, but had no effect in the *KRAS*WT model (Figure S1E, upper panel), and of these 21 siRNAs, those targeting *EFNA2*, *EPHA1*, *EFNA1*, *BIRC5*, *INPP4B*, and *STAT3* also sensitized to 5-FU treatment specifically in the *KRAS*MT cell line (Figure S1E, lower panel).

To rule out cell-line-specific effects, we carried out a secondary RNAi screen using three additional mutant *KRAS*-dependent CRC cell lines: LoVo (G13D), SW620 (G12V), and DLD-1 (G13D). Notably, only 16/77 siRNAs had a significant inhibitory effect on survival in all three of these cell line models, and these included genes involved in STAT3 signaling (*OSM*, *JAK1*, *JAK2*, and *STAT3*; Figure S1F). siRNA-mediated downregulation of each target gene was confirmed by real-time PCR (data not shown). Given the relevance of STAT3 signaling in CRC tumor development (Corvinus et al., 2005; Grivennikov et al., 2009), its association with adverse outcome in CRC, and the presence of multiple druggable targets in this pathway, we carried forward JAK1/2-STAT3 for further validation using three additional siRNA sequences and a second isogenic paired CRC model (*KRAS*MT [G13D] DLD1 and *KRAS*WT Dks-8). These experiments confirmed that RNAi-mediated inhibition of JAK1/2-STAT3 signaling reduced the viability of *KRAS*MT HCT116 and DLD-1 cells, but not their *KRAS*WT counterparts (Figure S1G).

STAT3 Regulates the Sensitivity of *KRAS*MT CRC to MEK Inhibitors and Chemotherapy

Based on the results from the RNAi screens, we next examined the effect of the clinically relevant MEK1/2 inhibitor AZD6244 and the chemotherapeutic agents 5-FU, oxaliplatin, and SN-38 on STAT3 activation. STAT3 phosphorylation (Y^{705}), but not total expression, was acutely increased in *KRAS*MT HCT116 cells in response to each agent (Figures 1A, S2A, and S2B). In contrast, AZD6244 or chemotherapy treatment had little impact on pSTAT3 levels in the *KRAS*WT model (Figures 1A and S2A). Similar effects were observed in a panel of *KRAS*MT and *KRAS*WT CRC cells and with three different MEK inhibitors (Figures 1B, S2C, and S2D). In addition, siRNAs against KRAS or ERK1/2 also significantly increased STAT3 phosphorylation in *KRAS*MT CRC cells, indicating that this is a common effect of inhibiting the MEK/ERK pathway in *KRAS*MT CRC (Figures 1C and 1D, left panel). Constitutive pSTAT3 levels were higher in *KRAS*MT HCT116 and DLD-1 cells compared with their isogenic WT clones; however, there was no clear pattern of pSTAT3 expression in a panel of nonmatched *KRAS*MT and *KRAS*WT CRC cells (Figure S2E).

These results suggested a role for STAT3 in mediating resistance to MEK-targeted agents and chemotherapy in *KRAS*MT CRC cells. To investigate this, we assessed the effect of STAT3 silencing on apoptosis induction by flow cytometry and western blotting for PARP cleavage and activation of caspase

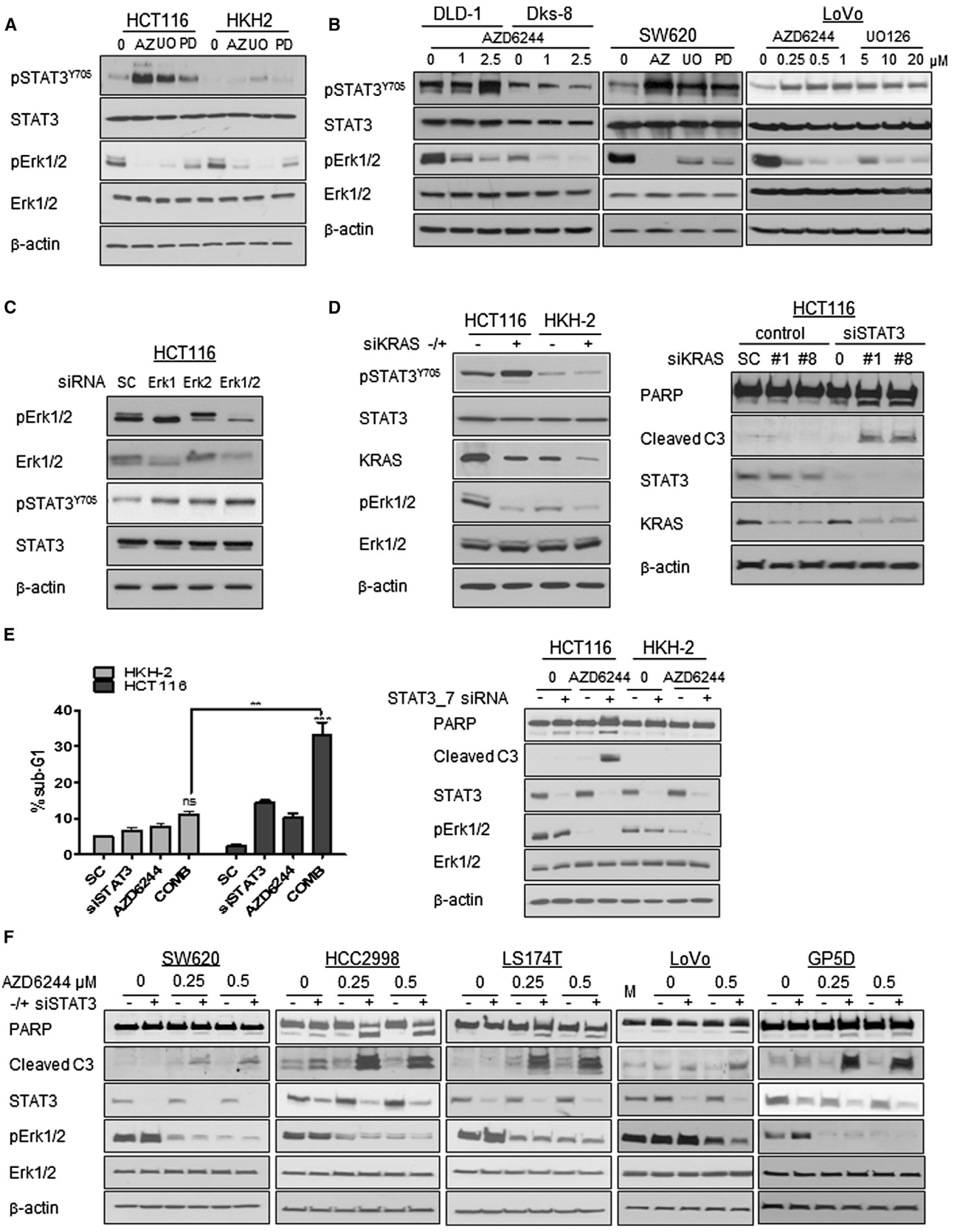

(legend on next page)

3. Cotreatment with STAT3 siRNA and KRAS siRNA or AZD6244 resulted in significant increases in apoptosis in the *KRAS*MT HCT116 cell line, but not in the *KRAS*WT daughter cell line (Figure 1D, right panel, and 1E). We extended these studies to include a panel of *KRAS*MT cells (SW620 *KRAS*G12V, HCC2998 *KRAS*A146T, LS174T *KRAS*G12D, LoVo *KRAS*G13D, and GP5D *KRAS*G12D). A significant increase in apoptosis was observed when *KRAS*MT cells were cotreated with AZD6244 and STAT3 siRNA (Figure 1F). Similar results were obtained for the combination of STAT3 siRNA with 5-FU, oxaliplatin, or SN-38 (Figure S2F). Collectively, these data indicate that STAT3 is an important survival pathway following RNAi-mediated or pharmacological blockade of the oncogenic KRAS-MEK signaling pathway and in response to clinically relevant cytotoxic agents in *KRAS*MT CRC.

JAK1 and JAK2 Regulate STAT3 Activation and Are Key Mediators of Resistance to MEK Inhibitors in *KRAS*MT CRC Cells

We next investigated the involvement of the upstream kinases JAK1 and JAK2 in regulating STAT3 activity and the survival of *KRAS*MT and *KRAS*WT CRC cells. Silencing of either JAK1 or JAK2 resulted in potent inhibition of constitutive STAT3 phosphorylation, and this was associated with an increase in PARP cleavage in the HCT116 cell line, but not in the *KRAS*WT isogenic clone (Figure 2A). Importantly, JAK1 or JAK2 silencing abrogated AZD6244-induced STAT3 activation and increased MEK inhibitor-induced apoptosis in *KRAS*MT, but not *KRAS*WT, HCT116 cells (Figures 2B, 2C, and S3A). Similar results were obtained in the panel of *KRAS*MT CRC cells (Figures 2D and 2E). Silencing of JAK2 had no effect on pJAK1 levels, but decreased both basal and MEKi-induced STAT3 activity (Figure 2F). However, RNAi against JAK1 decreased MEKi-induced increases in pJAK2 levels and resulted in more potent inhibition of both basal and MEKi-induced STAT3 activity compared with the effects of JAK2 silencing. This suggests that JAK1 and JAK2 cooperate to regulate the STAT3 survival response in response to MEKi.

Similar results were obtained with the JAK2 inhibitor TG101348, which also has inhibitory activity against JAK1 (Wernig et al., 2008). Treatment with TG101348 resulted in potent inhibition of $STAT3^{Y705}$ phosphorylation and induced apoptosis as indicated by increased PARP cleavage and caspase 3 processing in the *KRAS*MT cell line, but not the *KRAS*WT line (Figures 3A, S3B, and S3C). In addition, MEK inhibitor-induced STAT3 phosphorylation was associated with increased JAK2 phosphorylation that was completely abrogated upon cotreatment with TG101348, and this resulted in higher levels of apoptosis in *KRAS*MT HCT116 cells compared with the *KRAS*WT daughter cell line (Figure 3B). Of note, increased JAK1 phosphorylation following AZD6244 treatment was also abrogated following treatment with TG101348 (Figure 3B). Cell viability was significantly reduced in the *KRAS*MT HCT116 cell line compared with the *KRAS*WT daughter cell line following cotreatment with TG101348 and AZD6244 (Figure S3D). Calculation of combination index (CI) values confirmed a strong synergy between TG101348 and AZD6244 in the *KRAS*MT HCT116 cell line (Figure S3D, left panel). Importantly, similar results were obtained in a wider panel of *KRAS*MT (LS174T, SW620, LoVo, HCC2998, and GP5D) and *KRAS*WT (CACO-2, H630, LIM1215, and COLO320) CRC cell line models, with AZD6244 increasing STAT3 and JAK2 activity and synergizing with TG101348 in all *KRAS*MT models (Figures 3C and S3E), but not *KRAS*WT cells (Figure S3F). Moreover, similar results were obtained when TG101348 was combined with 5-FU, SN-38, or oxaliplatin in *KRAS*WT/*KRAS*MT CRC cells (Figures S3G–S3J). These results are also independent of the *PIK3CA* mutational status since 5/7 *KRAS*MT models have *PIK3CA* mutations (HCT116, HCC2998, LS174T, GP5D, and DLD-1), whereas SW620 and LoVo cells are *PIK3CA* (and *PTEN*) WT (Jhawer et al., 2008).

JAK Inhibitors Synergize with Both MEKi and Chemotherapy In Vivo

Based on the compelling in vitro evidence, we next assessed the therapeutic efficacy of combined JAK1/2 and MEKi in *KRAS*MT xenograft models using AZD6244 and the JAK1/2 inhibitor AZD1480 (Hedvat et al., 2009; Figure S4A). In agreement with the data obtained using TG101348, we found supra-additive increases in cell death when AZD1480 was combined with the MEK inhibitor AZD6244 or UO126 in the *KRAS*MT HCT116 cell line (Figure 4A, S4B, and S4C). Importantly, the MEKi/JAK inhibition (JAKi) combination led to a marked reduction in the growth of *KRAS*MT HCT116 xenografts compared with treatment with each agent individually (Figure 4B).

Figure 1. STAT3 Is Required for the Survival of *KRAS*MT CRC Cells

(A) HCT116 and HKH-2 cells were treated with 1 μM AZD6244 (AZ), 5 μM UO126 (UO), or 5 μM PD98059 (PD) for 24 hr, and STAT3 and Erk1/2 expression and activity levels were determined by western blotting (WB).

(B) DLD-1 and Dks-8 cells were treated with 1 and 2.5 μM AZD6244; SW620 cells were treated with 0.5 μM AZD6244, 2.5 μM UO126, or 5 μM PD98059; and LoVo cells were treated with the indicated doses of AZD6244 or UO126 for 24 hr. STAT3 and Erk1/2 expression and activity levels were determined by WB.

(C) HCT116 cells were transfected with 5 nM SC siRNA, Erk1 siRNA, Erk2 siRNA, or combined Erk1/Erk2 siRNA for 24 hr, and $pSTAT3^{Y705}$, STAT3, pErk1/2, and Erk1/2 levels were determined by WB.

(D) Left panel: expression of $pSTAT3^{Y705}$, STAT3, KRAS, pErk1/2, and Erk1/2 in HCT116 and HKH-2 cells transfected with 5 nM KRAS siRNA (siKRAS) for 24 hr. Right panel: HCT116 cells were transfected with 5 nM STAT3 siRNA (siSTAT3), 5 nM KRAS siRNA, or combined STAT3/KRAS siRNA for 24 hr, and expression of PARP, cleaved caspase 3 (C3), STAT3, and KRAS was determined by WB; #1 and #8 denote different KRAS siRNA sequences.

(E) HCT116 and HKH-2 cells were transfected with 5 nM STAT3 siRNA and cotreated with AZD6244 (0.5 μM) for 24 hr, and apoptosis was assessed by flow-cytometric analysis with propidium iodide (PI, left panel) and by WB for PARP and C3 cleavage (right panel). Error bars indicate SD of mean; two-way ANOVA; $^{***}p < 0.001$.

(F) *KRAS*MT SW620, HCC2998, LS174T, LoVo, and GP5D cells were transfected with 5 nM STAT3 siRNA and cotreated with AZD6244 for 24 hr, and apoptosis was assessed by WB for PARP and C3 cleavage. M, mock-transfection control.

See also Figures S1 and S2, and Tables S1–S3.

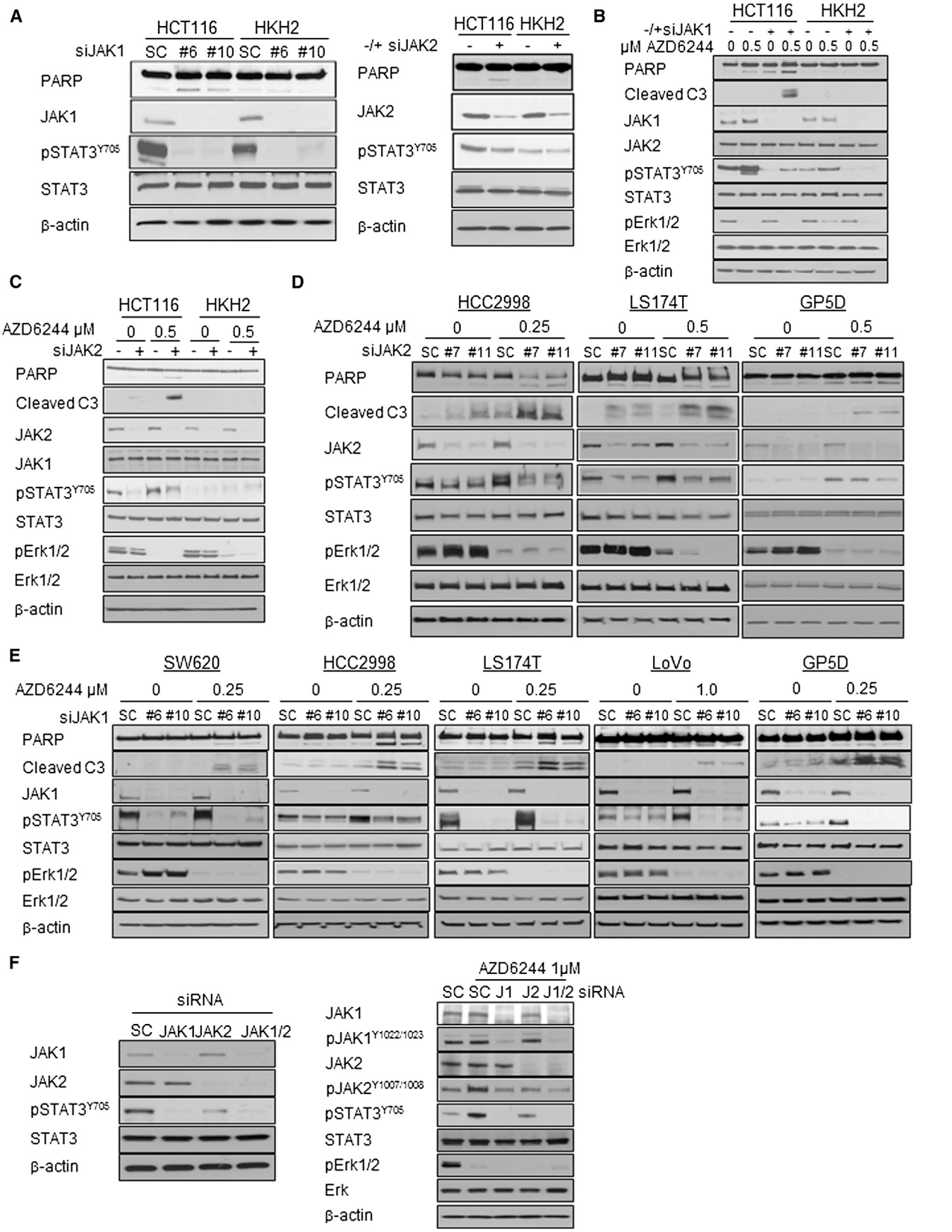

(legend on next page)

Moreover, the combined treatment was well tolerated, and in fact the body weight of mice treated in the combination arm actually increased (Figure 4C). Western blot analyses confirmed that ERK1/2 and STAT3 phosphorylation was inhibited following AZD6244 and AZD1480 treatment, respectively, in HCT116 xenografts, demonstrating the on-target effects of the inhibitors (Figure 4D). Importantly, treatment with AZD6244 resulted in significantly increased levels of pSTAT3 in *KRAS*MT HCT116 xenografts, and this was abrogated in xenografts cotreated with AZD1480. Moreover, caspase 3 cleavage was observed in the HCT116 tumors following treatment of AZD6244 alone and AZD6244 in combination with AZD1480, indicative of apoptosis induction (Figure 4D). Similar effects were observed in the *KRAS*MT (G12V) SW620 xenograft model; in particular, the combination treatment resulted in significant processing of caspase 3 compared with the individual treatments in this model (Figures 4E, 4F, and S4D). Cotreatment with AZD1480 and the clinically relevant combination of 5FU and oxaliplatin also resulted in apoptosis and a synergistic reduction of tumor growth in *KRAS*MT CRC in vitro and in vivo models (Figures 4G, 4H, and S4E). These results strongly suggest that JAK1/2-targeted agents may be highly effective combination partners for MEK1/2-targeted therapies or chemotherapy in *KRAS*MT CRC.

c-MET Is Activated following MEKi and Regulates JAK1/2 and STAT3

Mechanistically, no increase in shedding of interleukin-6 (IL-6), a key activator of STAT3 signal transduction, was found following AZD6244 treatment (data not shown). In addition, siRNA against IL-6 or a monoclonal antibody against IL-6 receptor did not affect basal or AZD6244-induced STAT3 activation (Figure S5A).

To further investigate the upstream mechanisms involved in AZD6244-induced STAT3 activation, we assessed the phosphorylation status of 42 receptor tyrosine kinases (RTKs) in *KRAS*MT HCT116 cells 24 hr following treatment with AZD6244 (Figure 5A, left panel). Notably, very few changes in RTK activation were observed following AZD6244 treatment; however, in addition to EGFR, HER2, and HER3, we found increased phosphorylation of the RTK c-MET. We next validated these array results by western blotting using phospho-specific EGFR, HER2, HER3, and c-MET antibodies that reflect the activation state of the receptors. Interestingly, basal phosphorylation of EGFR and particularly HER2 and HER3 was higher in *KRAS*WT cells (Figure S5B, left panel). The phosphorylation of these receptors increased moderately in HCT116 cells following treatment with AZD6244 (confirming the results of the RTK array analysis), but not in the HKH-2 cells (Figure S5B, left panel). However, basal and AZD6244-induced STAT3 phosphorylation was unaffected by treatment with dual EGFR/HER2 inhibitors (Figure S5B, right and lower panel), indicating that activation of STAT3 following MEKi is not driven by EGFR or HER2. Importantly, c-MET activation increased dramatically following treatment with AZD6244 in HCT116 cells, but *not* in HKH-2 cells (Figures 5A, right panel, and S5C). Similar results were obtained using siRNA against ERK1/2 and four different MEK1/2 targeted agents in several *KRAS*MT CRC models (Figure S5C). Moreover, incubation of HCT116 cells with the c-MET ligand recombinant hepatocyte growth factor (rHGF) resulted in significant increases in STAT3 phosphorylation (Figure S5D), demonstrating a clear link between c-MET and STAT3 in these cells.

To investigate directly the role of c-MET in regulating resistance to MEK1/2 inhibitors, we used c-MET siRNA and the c-MET/ALK inhibitor crizotinib. Notably, exposure of *KRAS*MT cells to crizotinib or c-MET siRNA abrogated MEKi-induced activation of STAT3 and resulted in significantly increased apoptosis (Figures 5B and S5E). In addition, we also observed synergistic increases in apoptosis when *KRAS*MT SW620, LoVo, LS174T, and GP5D cells were cotreated with AZD6244 and crizotinib (Figures 5C and S5F). Furthermore, AZD6244-induced activation of JAK1/2 and GAB1 (a key c-MET adaptor protein) was also inhibited by crizotinib in *KRAS*MT CRC cells (Figure 5D). Moreover, silencing of GAB1 abrogated AZD6244-induced JAK1 and STAT3 activation, indicating that this adaptor protein is involved in MET-induced JAK/STAT3 activation following MEKi (Figure S5G). Collectively, these results indicate that the AZD6244-induced JAK/STAT3 survival response is induced by c-MET.

We also investigated the effect of MEKi on JAK/STAT3 signaling and the upstream RTKs EGFR, HER2, HER3, and c-MET in *BRAF*MT VACO432, RKO, and LIM2405 cell lines. Similar to the data obtained in *KRAS*MT CRC cells, AZD6244 treatment resulted in acute increases in JAK2/STAT3 activity in all *BRAF*MT cell lines, but this was only associated with increases in c-MET, EGFR, and/or HER3 activity in VACO432 and RKO cells (Figure S5H).

Figure 2. *KRAS*MT CRC Cells Are Dependent on JAK1/2 for Survival

(A) Left panel: HCT116 and HKH-2 cells were transfected with 5 nM JAK1 siRNA (siJAK1) for 48 hr, and PARP, JAK1, pSTAT3^{Y705}, and STAT3 levels were determined by WB; #6 and #10 denote different JAK1 siRNA sequences. Right panel: HCT116 and HKH-2 cells were transfected with 5 nM JAK2 siRNA (siJAK2) for 48 hr, and PARP, JAK2, pSTAT3^{Y705}, and STAT3 levels were determined by WB.

(B) HCT116 and HKH2 cells were cotreated with 5 nM JAK1 siRNA and AZD6244, and PARP, cleaved C3, JAK1, JAK2, pSTAT3^{Y705}, STAT3, pErk1/2, and Erk1/2 levels were determined by WB.

(C) Expression of PARP, cleaved C3, JAK2, JAK1, pSTAT3^{Y705}, STAT3, pErk1/2, and Erk1/2 in HCT116 and HKH-2 cells transfected with JAK2 siRNA (5 nM) and cotreated with AZD6244 for 24 hr.

(D) HCC2998, LS174T, and GP5D cells were transfected with 5 nM JAK2 siRNA and cotreated with AZD6244 for 24 hr, and apoptosis was assessed by WB for PARP and C3 cleavage; #7 and #11 denote different JAK2 siRNA sequences.

(E) SW620, HCC2998, LS174T, LoVo, and GP5D cells were transfected with 5 nM JAK1 siRNA and cotreated with AZD6244 for 24 hr, and apoptosis was assessed by WB for PARP and C3 cleavage.

(F) Left panel: HCT116 cells were transfected with 10 nM JAK1 or JAK2 siRNA, or cotransfected with 10 nM JAK1 and JAK2 siRNA for 24 hr. Right panel: HCT116 cells were transfected with 10 nM JAK1 siRNA (J1) or JAK2 siRNA (J2), or cotransfected with 10 nM JAK1 and JAK2 siRNA (J1/2) and cotreated with AZD6244 for 24 hr. JAK1, pJAK1$^{Y1022/1023}$, JAK2, pJAK2$^{Y1007/1008}$, pSTAT3^{Y705}, and STAT3 levels were determined by WB.

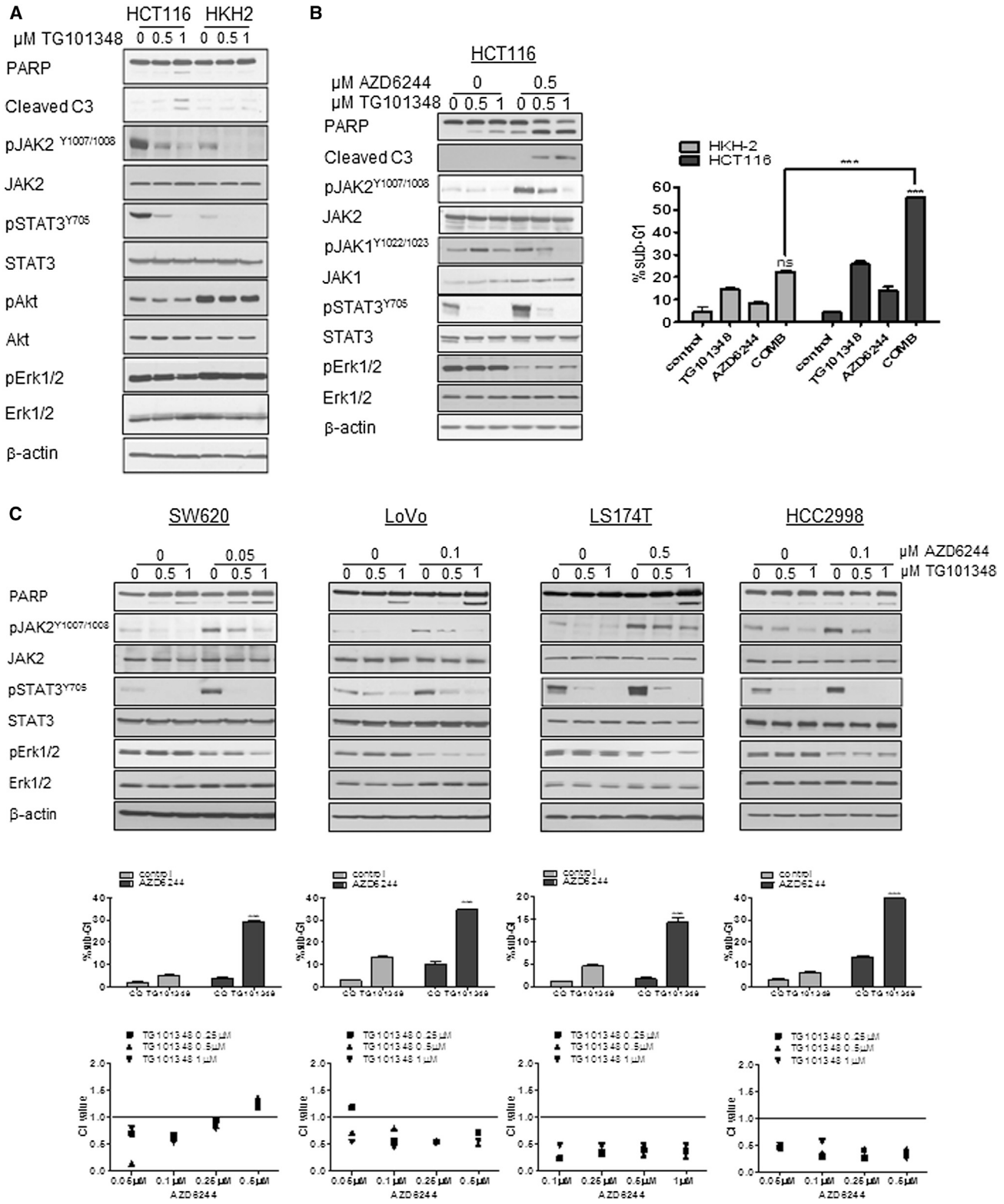

Figure 3. TG101348 and AZD6244 Result in Cell Death in a Panel of *KRAS*MT CRC Cells

(A) HCT116 and HKH-2 cells were treated with TG101348 for 24 hr, and PARP, cleaved C3, pJAK2$^{Y1007/1008}$, JAK2, pSTAT3^{Y705}, STAT3, pAkt, Akt, pErk1/2, and Erk1/2 levels were determined by WB.

(legend continued on next page)

Coinhibition of c-MET and MEK1/2 Inhibits the Growth of *KRAS*MT Xenograft Models

We next assessed the therapeutic efficacy of combined c-MET and MEK inhibition in *KRAS*MT HCT116 and SW620 xenograft models. Although both crizotinib and AZD6244 slowed tumor growth, the MET inhibition (METi)/MEKi combination led to a supra-additive reduction in growth in both *KRAS*MT xenograft models (Figures 6A, 6B, and S6A). Similar to our results with AZD1480, we found that AZD6244-induced STAT3 phosphorylation was inhibited in xenografts cotreated with crizotinib (Figures 6A and 6B). In addition, combined crizotinib/AZD6244 treatment resulted in high levels of caspase 3 activation in HCT116 and SW620 xenografts (Figure 6C). These findings indicate that c-MET-targeted agents may be highly effective when used in conjunction with MEK1/2-targeted therapies to treat *KRAS*MT CRC.

ADAM17-Mediated Cleavage Regulates c-MET Shedding in *KRAS*MT CRC

We next investigated the mechanism of MEK-inhibitor-induced c-MET activation. A number of reports have shown that c-Src can interact with and regulate the phosphorylation of a number of RTKs, such as c-MET and EGFR (Biscardi et al., 1999; Sen et al., 2011). Inhibition of Src using AZD0424 resulted in minor inhibition of MEKi-induced STAT3 phosphorylation, but had no effect on phosphorylation of c-MET (Figure S6B). We recently showed that oncogenic *KRAS* regulates the activity of the metalloprotease ADAM17 following chemotherapy treatment in a MEK/ERK-dependent manner (Van Schaeybroeck et al., 2011). In addition, we previously found decreased c-MET activation following ADAM17 overexpression in *KRAS*MT CRC models (Kyula et al., 2010). Importantly, we found that c-MET, JAK2, JAK1, and STAT3 activation were potently increased by *ADAM17* gene silencing, whereas silencing of the other major ADAMs did not significantly affect this c-MET/JAK/STAT3 signaling axis (Figure 7A, left panel). Furthermore, pharmacological inhibition of ADAM17 using the dual ADAM10/ADAM17 inhibitor GW280264X confirmed these results (Figures 7A, right panel, and S6C). Importantly, transient overexpression of exogenous ADAM17 resulted in complete inhibition of c-MET, JAK1/2, and STAT3 phosphorylation following MEKi treatment (Figure 7B).

ADAM17 can control the activity of growth factor receptors through the generation of soluble ligands or soluble receptors (Murphy, 2008). We could not detect the c-MET ligand HGF in the culture medium of CRC cells, and anti-HGF neutralizing antibodies had no effect on basal or MEKi-induced STAT3 activation (Figure S6D and data not shown). However, we found significant decreases in soluble ("decoy") c-MET in culture medium of *KRAS*MT CRC cells following treatment with MEKi, ADAM17 siRNA, and two different ADAM17 inhibitors (Figures 7C, left panel, 7D, and S6E). In addition, significant increases in soluble c-MET were found in ADAM17-overexpressing cells, and this correlated with almost complete attenuation of c-MET activation (Figure 7C, middle and right panels). Notably, highly significant decreases in soluble human c-MET were detected in the serum of mice following 14 days treatment with AZD6244 (Figure 7E). Importantly, overexpression of ADAM17 increased soluble c-MET in the serum (Figure 7E, middle panel). In addition, transient overexpression of decoy/soluble MET inhibited c-MET activation in response to MEKi in *KRAS*MT HCT116 cells (Figure 7F, upper panel).

Transfer of conditioned medium from ADAM17-overexpressing HCT116 cells to untransfected HCT116 cells resulted in inhibition of c-MET activation. Importantly, when total MET expression was downregulated with siRNA in the ADAM17-overexpressing cells, the conditioned medium not only failed to inhibit c-MET activation but actually induced an increase in activation. This result indicates that ADAM17 promotes shedding of soluble MET that inhibits the activation of c-MET *and* that other ligands and receptors that can crosstalk with c-MET (for example, AXL) are activated by ADAM17 in the absence of soluble MET (Figure 7F, lower panel).

The cytoplasmic domain of ADAM17 contains binding sites for SH3 domain-containing structures and phosphorylation sites for serine-threonine and/or tyrosine kinases (Seals and Courtneidge, 2003). In addition to PKC signaling, several other signaling pathways can regulate shedding of ADAM17 substrates, including stimulation of GPCR (Hart et al., 2005; Lemjabbar-Alaoui et al., 2011). We further demonstrated that ADAM17 directly interacts with the MEK downstream targets ERK1/2 (Figure 7G, upper panel). In addition, an ADAM17 activity assay carried out on ERK1/2-associated proteins demonstrated that ADAM17 activity was significantly reduced following treatment with a MEK inhibitor (Figures 7H and S6F). These data indicate that ERK1/2 is in a complex with ADAM17, providing a direct mechanistic link between MEK and ADAM17.

In contrast to MEKi, no changes in soluble MET or c-MET activation were found following treatment of *KRAS*MT cells with 5-FU (Figure S6G), suggesting an alternative mechanism of JAK/STAT3 activation in response to this agent. We found instead that IGF-1R regulates 5-FU-induced STAT3 activity in *KRAS*MT CRC cells and this correlated with enhanced PARP cleavage when IGFR1-depleted cells were treated with 5-FU (Figures S6G and S6H).

DISCUSSION

KRAS mutational status was the first predictive biomarker to be integrated into clinical practice for advanced CRC (Van Cutsem et al., 2011). The high prevalence and therapeutic challenges

(B) Left panel: PARP, cleaved C3, pJAK2$^{Y1007/1008}$, JAK2, pJAK1$^{Y1022/1023}$, JAK1, pSTAT3^{Y705}, STAT3, pErk1/2, and Erk1/2 levels in HCT116 cells cotreated with AZD6244 and TG101348 for 24 hr. Right panel: HCT116 and HKH-2 cells were cotreated with TG101348 (0.5 μM) and AZD6244 (0.5 μM) for 24 hr and apoptosis was assessed by flow-cytometric analysis with PI.

(C) Upper panel: PARP, pJAK2$^{Y1007/1008}$, JAK2, pSTAT3^{Y705}, STAT3, pErk1/2, and Erk1/2 levels in SW620, LoVo, LS174T, and HCC2998 *KRAS*MT cells following cotreatment of TG101348 with AZD6244. Middle panel: flow-cytometric analysis of apoptosis following cotreatment of 1 μM TG101348 with AZD6244 (0.05 μM for SW620, 0.5 μM for LS174T and LoVo, and 0.1 μM for HCC2998) for 24 hr. Error bars indicate SD of mean; two-way ANOVA; ***$p < 0.001$. Lower panel: SW620, LS174T, LoVo, and HCC2998 cells were cotreated with TG101348 and AZD6244 for 72 hr. CI values were calculated using Calcusyn v2.0.

See also Figure S3.

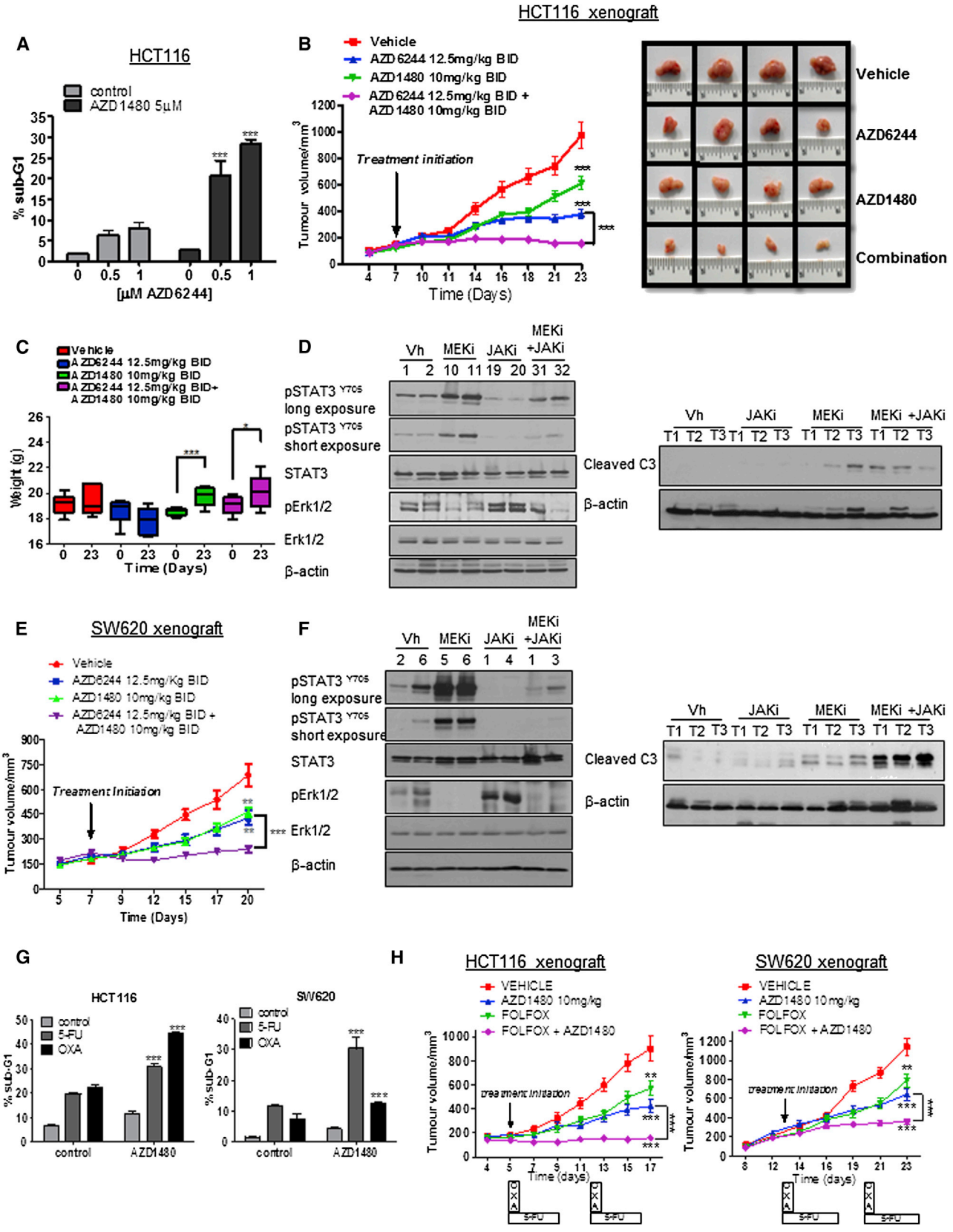

(legend on next page)

posed by *KRAS* mutations led to the exponential growth of translational research specifically aimed at targeting the survival of *KRAS* mutated tumors. Inhibition of MEK1/2 constitutes an attractive treatment strategy for *KRAS*MT CRC; however, acute activation of prosurvival pathways and other adaptive resistance mechanisms, such as amplification of the *KRAS* driver oncogene (Little et al., 2011), result in resistance to this class of agent and may limit its success in the clinic. Indeed, we found that MEK inhibitor monotherapy was relatively ineffective at inducing apoptosis in *KRAS*MT CRC models (Figure 2).

Constitutive activation of STAT3 is prevalent in a variety of tumors, including breast and prostate cancers (Garcia et al., 2001; Mora et al., 2002). With regard to CRC, a number of studies have shown that activated STAT3 plays an important role in enhanced colorectal tumor growth (Corvinus et al., 2005) and colitis-associated tumorigenesis (Grivennikov et al., 2009). Importantly, a recent study demonstrated that high tumor STAT3 activation is associated with peritumoral lymphocytic reaction and adverse outcome in CRC, suggesting its potential as a therapeutic target in this disease setting (Morikawa et al., 2011).

In the current study, we used a systems biology approach that incorporates in vitro, in vivo, clinical, and publicly available gene-expression data to identify pathways that are uniquely required in oncogenic *KRAS*-driven CRC and are also mediators of resistance to MEKi and chemotherapy treatment in this molecular subset of the disease. Pathway analyses identified a number of biological processes that were potentially central to the survival of *KRAS*MT CRC, including JAK/STAT signaling. Treatment with a range of MEK inhibitors and chemotherapeutic agents resulted in acute increases in STAT3 phosphorylation, which was significantly higher in *KRAS*MT CRC cells compared with *KRAS*WT cells. Multiple RNAi screens using several siRNA sequences against STAT3, JAK1, and JAK2, and multiple cell line models revealed that JAK1, JAK2, and STAT3 are important for maintaining the viability of *KRAS*MT, but not *KRAS*WT, cells and are critical mediators of resistance to MEKi and chemotherapy (5-FU, SN-38, and oxaliplatin) treatment in *KRAS*MT CRC. Moreover, by using selective inhibitors of JAK2 or a pan-JAK1/2 inhibitor, we further demonstrated the differential dependency of *KRAS*MT and *KRAS*WT cells on STAT3 for survival, particularly in the context of cotreatment with MEK inhibitors.

The importance of JAK1/2 and STAT3 as mediators of acute resistance to MEK1/2 inhibitors was demonstrated in vivo, where combined treatment of *KRAS*MT CRC xenografts with the JAK1/2 inhibitor AZD1480 and the MEK1/2 inhibitor AZD6244 blocked AZD6244-induced STAT3 activation and resulted in supra-additive reductions in tumor growth and marked induction of apoptosis. Collectively, these results indicate that inhibitors of the JAK1/2-STAT3 pathway in conjunction with MEKi could be a treatment strategy for *KRAS*MT CRC tumors. In addition, we also demonstrated that inhibition of the JAK1/2-STAT3 pathway in conjunction with standard chemotherapy (5FU and oxaliplatin) was highly effective at blocking the growth of *KRAS*MT CRC xenografts, suggesting that this combination is another potential treatment strategy for this molecular subgroup of CRC.

Mechanistically, we found that the RTK c-MET regulated the JAK1/2-STAT3-mediated survival response in *KRAS*MT CRC cells following AZD6244 treatment. Notably, our initial pathway analyses carried out to identify potential *KRAS* oncogene addiction targets and mechanisms of resistance to MEK inhibitors identified c-MET signaling (Figure S1B). Importantly, combined treatment of *KRAS*MT xenograft models with the c-MET inhibitor crizotinib and AZD6244 blocked AZD6244-induced STAT3 activation in vivo and resulted in supra-additive reductions in tumor growth and highly significant increases in apoptosis induction. This study shows that combined c-METi/MEKi could be a promising treatment strategy for *KRAS*MT CRC patients.

In contrast to a recent study by Prahallad et al. (2012), we did not observe involvement of the phosphatase CDC25C in regulating the feedback activation of c-MET, JAK1/2, and STAT3 in the context of MEKi treatment (data not shown). Previous findings, including data from our lab, have identified a role for c-Src in regulating feedback activation of EGFR and HER2 following cytotoxic drug treatment (Van Schaeybroeck et al., 2008). However, we did not find that c-Src was involved in mediating MEKi-induced c-MET activation. In agreement with our previous data showing that oncogenic *KRAS* regulates ADAM17 activity and EGFR-ligand shedding in a

Figure 4. The Combination of AZD1480 with AZD6244 or Chemotherapy Induces Tumor Regression in *KRAS*MT CRC In Vivo Models

(A) HCT116 cells were cotreated with AZD6244 and AZD1480 for 24 hr and apoptosis was assessed by flow-cytometric analysis with PI. Error bars indicate SD of mean; two-way ANOVA; ***$p < 0.001$.

(B) Left panel: growth rate of HCT116 xenografts in BALB/c Nude mice treated with vehicle, AZD6244, AZD1480, or combined AZD6244/AZD1480 treatment. Differences in growth were determined by Student's t test and by calculating subsequent p values (***$p < 0.001$). Error bars indicate SD of mean; n = 8 per group. Right panel: gross images showing representative cases treated with vehicle, AZD6244, AZD1480, or AZD6244 with AZD1480.

(C) Body weights of mice in the different treatment groups. Differences were determined using Student's t test and by calculating p values (*$p < 0.05$; ***$p < 0.001$).

(D) WB analysis of $pSTAT3^{Y705}$, STAT3, pErk1/2, Erk1/2, and cleaved C3 in HCT116 vehicle (Vh)-, AZD6244 (MEKi)-, AZD1480 (JAKi)-, and AZD6244/AZD1480 (MEKi+JAKi)-treated xenografts.

(E) Growth rate of SW620 xenografts in BALB/c Nude mice. Mice were treated with vehicle, AZD6244, AZD1480, or combined AZD6244/AZD1480 treatment. Differences in growth were determined using Student's t test and by calculating subsequent p values (**$p < 0.01$, ***$p < 0.001$). Error bars indicate SD of mean; n = 8 per group.

(F) WB analysis of $pSTAT3^{Y705}$, STAT3, pErk1/2, Erk1/2, and cleaved C3 in SW620 vehicle (Vh)-, AZD6244 (MEKi)-, AZD1480 (JAKi)-, and AZD6244/AZD1480-treated xenografts.

(G) Flow-cytometric analysis of apoptosis following cotreatment of 0.5 μM AZD1480 with 5-FU (5 μM and 10 μM in HCT116 and SW620, respectively) or 1 μM OXA. Error bars indicate SD of mean; two-way ANOVA; ***$p < 0.001$.

(H) Growth rate of HCT116 and SW620 xenografts in BALB/c Nude mice treated with vehicle, 5-FU/oxaliplatin (FOLFOX; 5-FU 15 mg/kg/d and oxaliplatin [OXA] 2 mg/kg), AZD1480, or combined FOLFOX/AZD1480 treatment. Differences in growth were determined using Student's t test and by calculating subsequent p values (**$p < 0.01$; ***$p < 0.001$); n = 8 per group.

See also Figure S4.

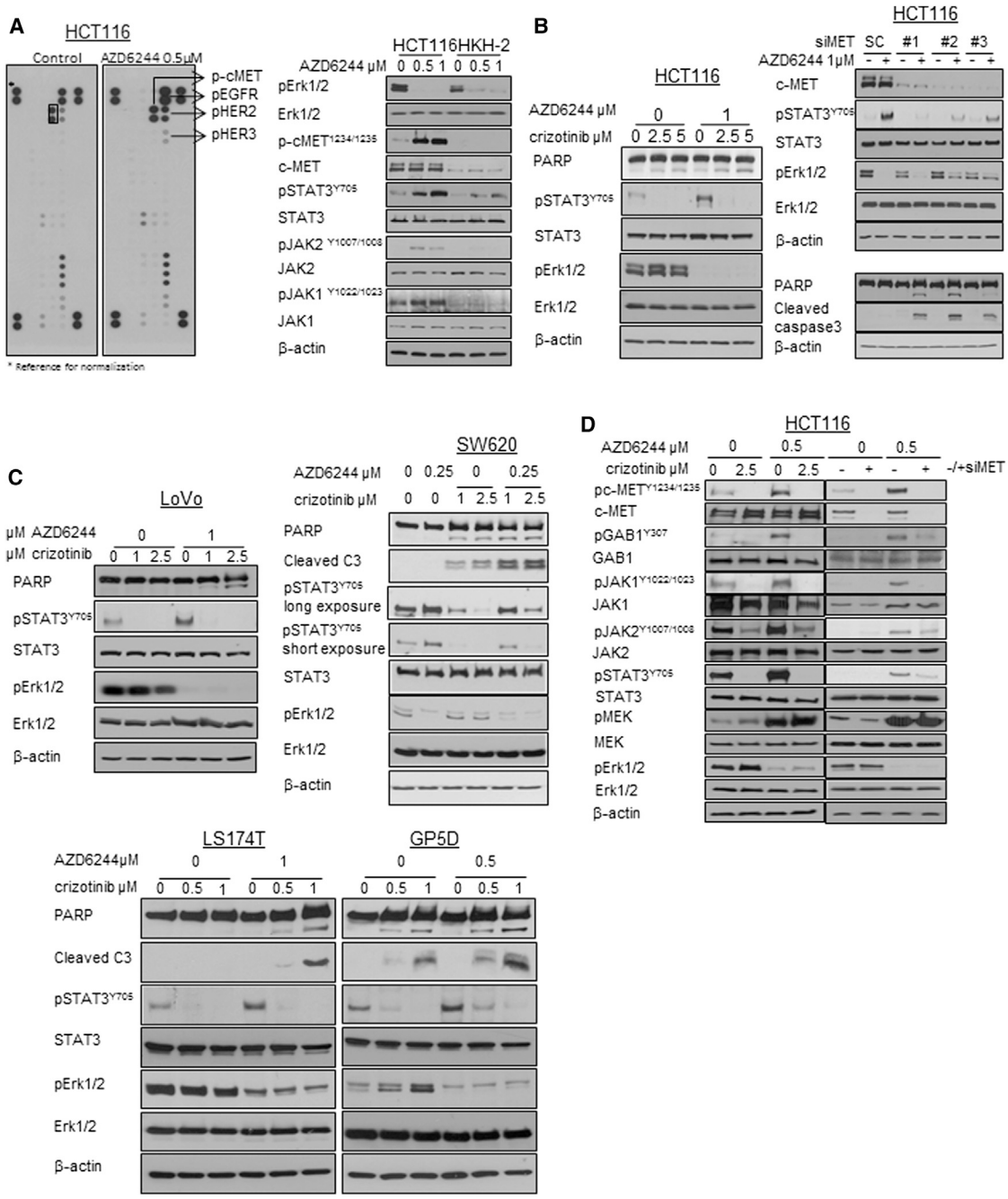

Figure 5. MEK1/2 Inhibition Results in Increased Activity of Survival Receptors Such as HER1/2/3 and c-MET

(A) Left panel: Human phospho-RTK array in HCT116 cells. HCT116 cells were treated with AZD6244 for 24 hr followed by protein extraction. Right panel: HCT116 and HKH-2 cells were treated with AZD6244 for 24 hr, and pErk1/2, Erk1/2, p-cMET$^{Y1234/Y1235}$, c-MET, pSTAT3^{Y705}, STAT3, pJAK2$^{Y1007/1008}$, JAK2, pJAK1$^{Y1022/1023}$, and JAK1 levels were determined by WB.

(B) Left panel: HCT116 cells were cotreated with crizotinib and AZD6244 for 24 hr, and PARP, pSTAT3^{Y705}, STAT3, pErk1/2, and Erk1/2 expression levels were determined by WB. Right panel: HCT116 cells were transfected with 5 nM c-MET siRNA and cotreated with 1 μM AZD6244 for 24 hr, and c-MET, pSTAT3^{Y705}, STAT3, pErk1/2, Erk1/2, cleaved C3, and PARP levels were determined by WB. cMET#1, cMET#2, and cMET#3 denote different c-MET siRNA sequences.

(C) LoVo, SW620, LS174T, and GP5D cells were cotreated with crizotinib and AZD6244 for 24 hr, and PARP, cleaved C3, pSTAT3^{Y705}, STAT3, pErk1/2, and Erk1/2 levels were determined by WB.

(D) HCT116 cells were cotreated with AZD6244 and crizotinib or 5 nM c-MET siRNA for 24 hr, and p-c-MET$^{Y1234/Y1235}$, c-MET, pGAB1^{Y307}, GAB1, pJAK2$^{Y1007/1008}$, JAK2, pJAK1$^{Y1022/1023}$, JAK1, pSTAT3^{Y705}, STAT3, pMEK, MEK, pErk1/2, and Erk1/2 levels were determined by WB.

See also Figure S5.

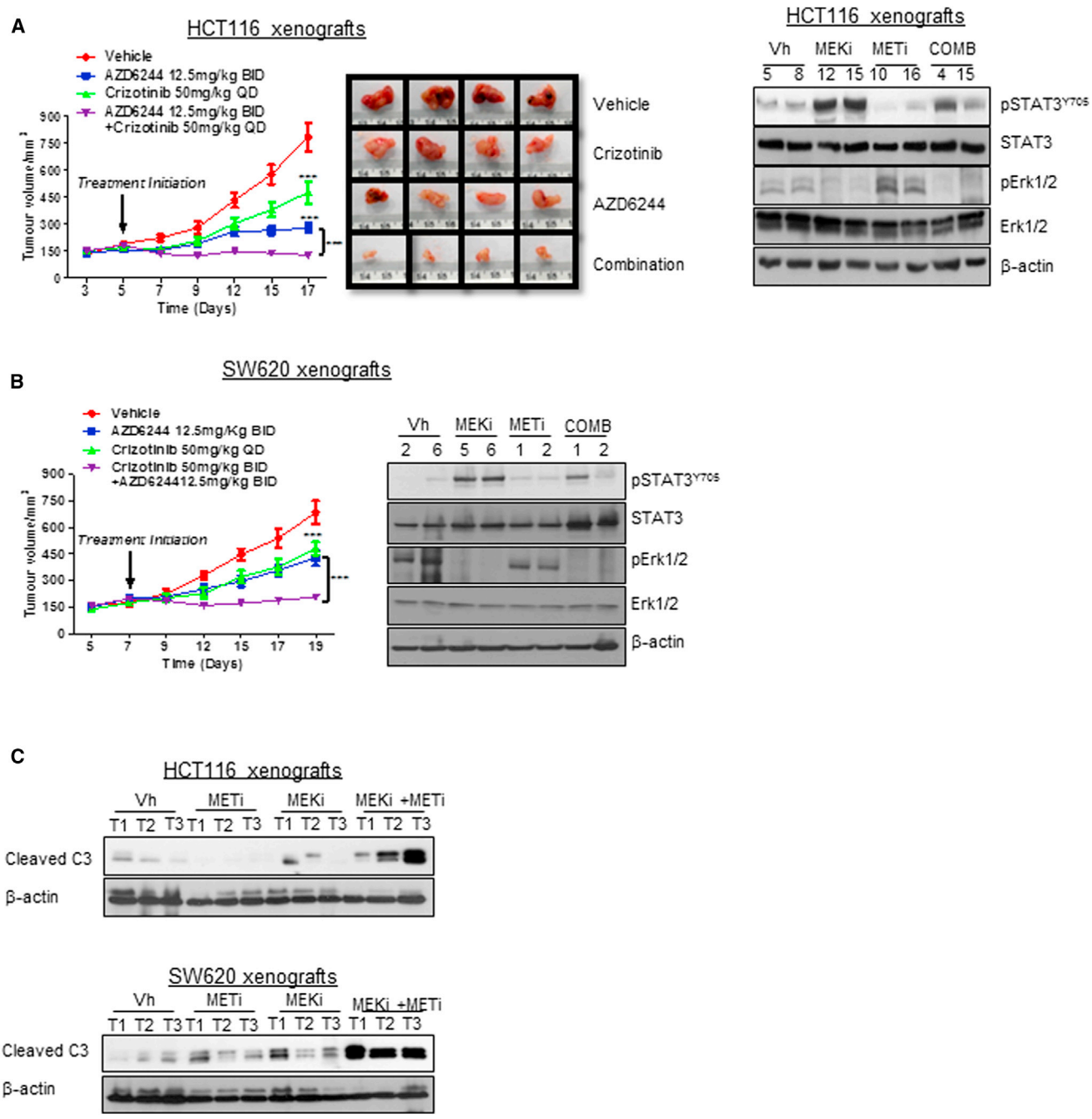

Figure 6. Combined c-MET and MEK Inhibition Results in a Synergistic Reduction in the Growth of *KRAS*MT CRC Xenograft Models

(A) Left panel: the growth rate of HCT116 xenografts in BALB/c Nude mice treated with vehicle, AZD6244, crizotinib, or combined AZD6244/crizotinib treatment. Differences in growth were determined using Student's t test and by calculating subsequent p values (***$p < 0.001$). Error bars indicate SD of mean; n = 8 per group. Middle panel: gross images showing representative cases treated with vehicle, crizotinib, AZD6244, or AZD6244 with crizotinib. Right panel: WB analysis of $pSTAT3^{Y705}$, STAT3, pErk1/2, and Erk1/2 in HCT116 vehicle (Vh)-, AZD6244 (MEKi)-, crizotinib (METi)-, and AZD6244/crizotinib (COMB)-treated xenografts.

(B) Left panel: growth rate of SW620 xenografts in BALB/c Nude mice treated with vehicle, AZD6244, crizotinib, or combined AZD6244/crizotinib treatment. Differences in growth were determined using Student's t test and by calculating subsequent p values (***$p < 0.001$). Error bars indicate SD of mean; n = 8 per group. Right panel: WB analysis of $pSTAT3^{Y705}$, STAT3, pErk1/2, and Erk1/2 in SW620 vehicle-, AZD6244 (MEKi)-, crizotinib (METi)-, and AZD6244/crizotinib (COMB)-treated xenografts.

(C) WB analysis of cleaved C3 in HCT116 and SW620 vehicle-, AZD6244 (MEKi)-, crizotinib (METi)-, and AZD6244/crizotinib (MEKi+METi)-treated xenografts.

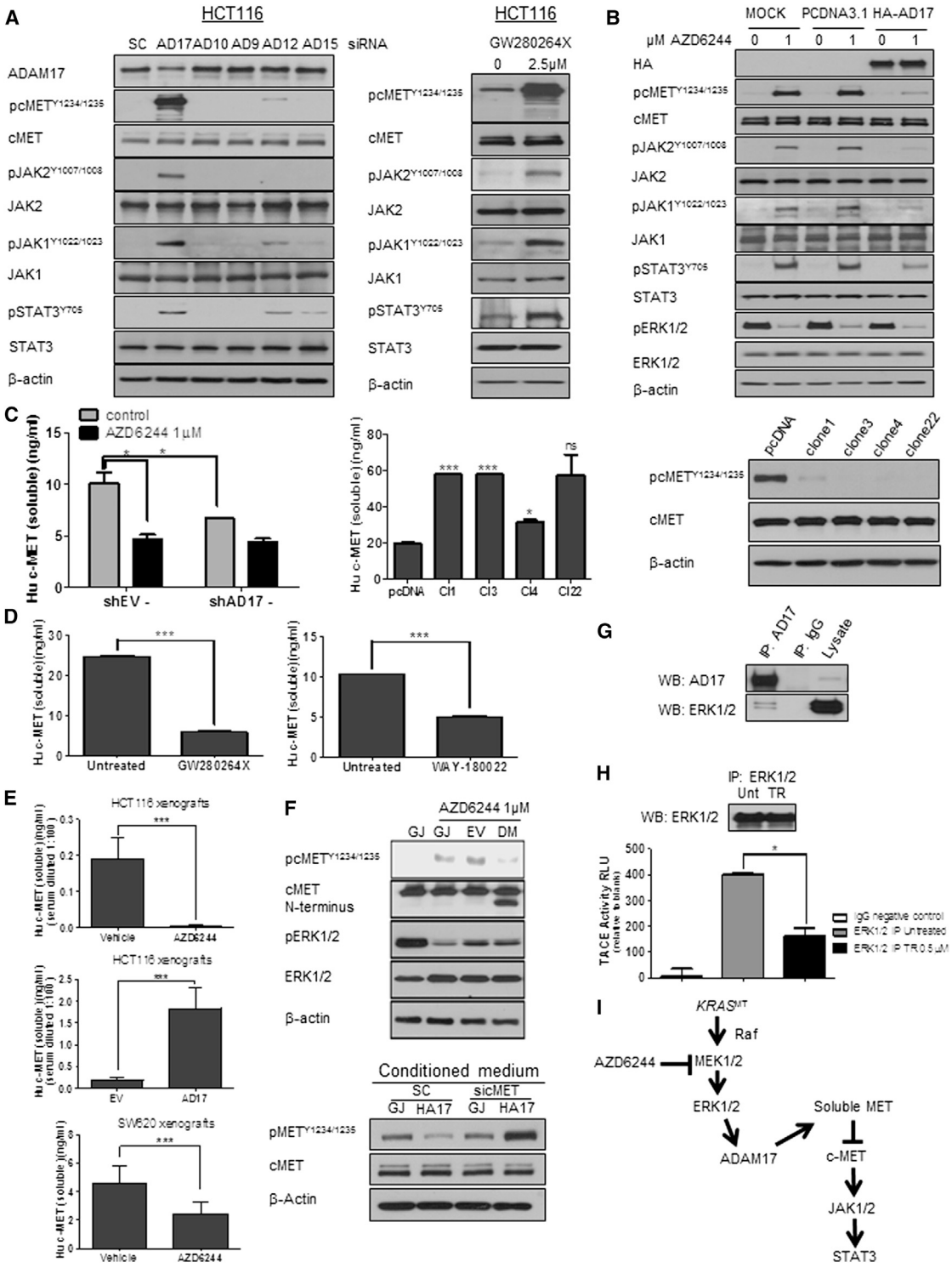

Figure 7. ADAM17 Mediates c-MET Shedding and Activation in *KRAS*MT CRC Cells

(A) Left panel: HCT116 cells were transfected with 10 nM ADAM17 (AD17), ADAM10 (AD10), ADAM9 (AD9), ADAM12 (AD12), ADAM15 (AD15), or 10 nM SC for 24 hr. Right panel: HCT116 cells were treated with GW280264X for 24 hr. ADAM17, pcMET$^{Y1234/1235}$, cMET, pJAK2$^{Y1007/1008}$, JAK2, pJAK1$^{Y1022/1023}$, JAK1, pSTAT3^{Y705}, and STAT3 levels were determined by WB.

(B) Expression of HA, pcMET$^{Y1234/1235}$, cMET, pJAK2$^{Y1007/1008}$, JAK2, pJAK1$^{Y1022/1023}$, JAK1, pSTAT3^{Y705}, STAT3, pErk1/2, and Erk1/2 in HCT116 cells transiently transfected with EV (PCDNA 3.1) or HA-ADAM17 expression construct for 12 hr followed by treatment with AZD6244 for 24 hr.

(legend continued on next page)

MEK/ERK-dependent manner, we now show that ERK1/2 interacts with ADAM17 and that ADAM17 regulates MEK inhibitor-induced activation of c-MET/JAK/STAT3 in *KRAS*MT models. Soluble HGF was not detected in the culture medium of *KRAS*MT cell line models; however, we found that MEK and ADAM17 regulated the levels of soluble decoy MET and thus MET activation in *KRAS*MT CRC models in vitro and in vivo. Soluble/decoy MET is a natural antagonist of c-MET, and some studies have indicated that soluble/decoy MET levels correlate with total cellular c-MET expression levels (Athauda et al., 2006). The use of decoy/soluble MET is a strategy that is currently being developed to inhibit c-MET (Comoglio et al., 2008), and other studies have shown that decoy/soluble MET (or recombinant Sema, c-MET's N terminus domain) can inhibit both HGF-dependent and -independent receptor activation, with the latter effect being mediated by its ability to interfere with c-MET homodimerization (Kong-Beltran et al., 2004; Michieli et al., 2004). These studies have also shown more significant decreases in tumor volume and metastatic spread following treatment with soluble decoy c-MET compared with HGF inhibition in an in vivo model (Michieli et al., 2004). We also found that transiently overexpressing decoy/soluble inhibited c-MET activation in response to MEKi in *KRAS*MT cells. Overall, our results suggest that by cleaving c-MET to its soluble form, ADAM17 normally represses c-MET/JAK/STAT3 signaling; however, when MEK-ERK signaling is inhibited, ADAM17 activity is decreased, resulting in increased c-MET/JAK/STAT3 signaling that promotes tumor survival (Figure 7I). Not unexpectedly, we found that the mechanisms of MEK- and chemotherapy-induced STAT3 activation in *KRAS*MT CRC cells are different, with initial studies suggesting that IGF-1R may be important for regulating STAT3 activation following treatment with 5-FU.

Our previous studies and those of others have shown the importance of ADAM17 as a major EGFR-HER3 ligand sheddase, and demonstrated that inhibiting ADAM17 resulted in growth inhibition and decreases in pERK1/2 and/or pAKT signaling (Kyula et al., 2010; Merchant et al., 2008; Zhou et al., 2006). We have also shown that chemotherapy treatment results in acute increases in ADAM17 and EGFR activity, and that ADAM17 plays an important role in resistance to chemotherapy treatment in CRC (Kyula et al., 2010). All of these studies would indicate that ADAM17 inhibition in conjunction with standard chemotherapy agents could be a treatment strategy for CRC and NSCLC, in particular in EGFR-dependent tumors. However, in this study, we found that ADAM17 negatively regulates c-MET signaling by increasing the levels of soluble MET. This suggests that ADAM17 plays a role in maintaining an epithelial morphology by promoting EGFR family signaling and repressing the cell migratory potential and EMT by suppressing c-MET signaling. Furthermore, this suggests c-MET activation as a potential mechanism of resistance not only to MEK1/2 inhibitors but also to ADAM17 inhibitors in *KRAS*MT CRC, which could explain at least to some extent the lack of clinical efficacy of broad-spectrum MMP inhibitors in CRC (Nemunaitis et al., 2000). Our results would therefore suggest that combination therapies of ADAM17 and c-MET inhibitors would be more clinically effective in *KRAS*MT CRC.

In conclusion, using a unique systems biology approach, we have identified a druggable mechanism of resistance to MEK inhibitors in *KRAS*MT CRC mediated by c-MET via JAK1/2-STAT3 that is acutely induced as a consequence of suppression of MEK-dependent, ADAM17-mediated shedding of the soluble decoy MET receptor. From a clinical perspective, our data provide a preclinical rationale for initiating phase I studies of MEK inhibitors with either c-MET or JAK inhibitors in second-line treatment or in the interval following first-line chemotherapy treatment of patients with *KRAS*MT metastatic CRC. Consequently, we are initiating the first clinical trial (FP-7: 602901-2) to examine the effectiveness of combined treatment with MEK and MET inhibitors in *KRAS*MT CRC patients. Our results also suggest that combinations of JAK1/2 inhibitors and standard chemotherapy (5-FU plus oxaliplatin, "FOLFOX") may be effective against *KRAS*MT metastatic CRC.

EXPERIMENTAL PROCEDURES

See Supplemental Experimental Procedures for detailed protocols.

In Vivo Samples for Microarray Analysis

In vivo studies were done as previously described (Van Schaeybroeck et al., 2011). Excised tumors from vehicle (methocel/polysorbate buffer)- and

(C) Left panel: HCT116 cells were transfected with 1 μg ADAM17 (shAD17) shRNA or 1 μg EV (shEV) for 4 hr and then treated with AZD6244 for 24 hr. Soluble c-MET in the medium was measured using a c-MET (soluble) ELISA kit. Middle panel: soluble c-MET levels in culture medium of pcDNA 3.1 and HA-ADAM17 stable clones (ADcl1, ADcl3, ADcl4, and ADcl22) were measured by ELISA. Right panel: levels of pcMET$^{Y1234/1235}$ and cMET in pcDNA 3.1 and HA-ADAM17 stable clones.

(D) Soluble c-MET ELISA in HCT116 cells treated with 5 μM of the ADAM17 inhibitor GW280264X or WAY-180022 for 24 hr.

(E) Upper panel: human soluble c-MET levels in serum from BALB/c Nude mice with HCT116 xenografts 14 days following treatment initiation with vehicle or AZD6244. Middle panel: human soluble c-MET levels in serum from BALB/c Nude mice with EV (pcDNA 3.1) and HA-ADAM17 clone 4 xenografts. Lower panel: human soluble c-MET levels in serum from BALB/c Nude mice with SW620 xenografts 14 days following treatment initiation with vehicle or AZD6244.

(F) Upper panel: expression of pcMET$^{Y1234/1235}$, cMET, pErk1/2, and Erk1/2 in HCT116 cells transiently transfected with empty vector (EV) or decoy MET (DM) expression construct for 12 hr followed by treatment with AZD6244 for 24 hr (GJ, gene juice). Lower panel: HCT116 cells were transiently transfected with HA-ADAM17 (HA17) expression construct or GJ for 12 hr followed by transfection with 10 nM cMET siRNA (sicMET) or SC for 24 hr. New HCT116 cells were seeded overnight and the medium from these cells was removed and replaced with conditioned medium of GJ-SC, HA17-SC, GJ-sicMET, or HA17-sicMET transfected HCT116 cells.

(G) Lysates from HA-ADAM17 stable clone 3 were immunoprecipitated with anti-ADAM17 or control IgG antibodies and then immunoblotted (WB) for ERK1/2 or ADAM17 (AD17). ERK1/2 and ADAM17 expression was also detected in control lysate of HCT116 cells.

(H) Lysates from HCT116 cells transfected with HA-ADAM17 expression construct, untreated or treated with 0.5 μM trametinib (TR), were immunoprecipitated with total ERK1/2 or control IgG antibodies and ADAM17 activity was measured using a fluorometric assay. ERK1/2 expression was determined by WB. Error bars indicate SD of mean; Student's t test; *$p < 0.05$, ***$p < 0.001$.

(I) Schematic overview of the mechanism of cMET/JAK/STAT3 activation following MEKi treatment.

Related to Figure S6.

AZD6244-treated *KRAS*MT HCT116 and isogenic *KRAS*WT HKH-2 xenografts were used for gene-expression profiling.

In Vivo Samples for Human c-MET (Soluble) ELISA

In vivo studies were done as previously described (Van Schaeybroeck et al., 2011). Serum was collected from vehicle- and AZD6244-treated EV and HA-ADAM17 xenografts, and human c-MET (soluble) was analyzed according to the ELISA kit instructions (Invitrogen).

Patient Samples

We collected 40 formalin-fixed, paraffin-embedded colorectal primary tumors from patients who had received first-line 5-FU/irinotecan treatment for advanced disease. All identifiable details from their clinical and histopathological information were anonymized and the study was approved by the Belfast HSC Trust Research Office and the Regional Ethics Committee for Northern Ireland. Hematoxylin and eosin-stained sections were generated and each tissue section had a minimum of 50% tumor cells. RNA and DNA were extracted from these samples for microarray profiling and *KRAS* mutational analysis, respectively.

siRNA Plate Analysis

siRNA screening was performed as described previously (Allen et al., 2012). Transfection conditions were optimized using a siRNA with a known effect on cell survival (c-FLIP). All Stars negative control (QIAGEN) and All Stars Death control (QIAGEN) were used as nontargeting and positive controls, respectively. KRAS siRNA and STK33 siRNA (Scholl et al., 2009) were used as KRAS oncogenic addiction controls. However, the status of STK33 as a true RAS synthetic lethal has been widely questioned (Babij et al., 2011).

In Vivo Studies

In vivo studies were conducted as previously described (Kyula et al., 2010). AZD6244 12.5 mg/kg/bid, AZD1480 10 mg/kg/bid p.o., and crizotinib 50 mg/kg/qd were administered by oral gavage. The control groups received vehicle (methocel/polysorbate buffer). In the combination groups, AZD6244 was administered together with AZD1480 or crizotinib. Each treatment group contained eight animals. Two hours following the final dosing, the mice were sacrificed and tumor tissue was excised and snap-frozen in liquid nitrogen for immunoblotting. The Animals (Scientific Procedures) Act 1986, 2010 EU Directive 2010/63/EU, and UKCCCR Guidelines were followed at all times (project license number PPL2704).

Statistical Analysis

All t tests and two-way ANOVAs were calculated using the GraphPad software (Prism4). Two-way ANOVA was used to determine the significance of change in the levels of apoptosis between different treatment groups. All changes in levels of apoptosis that are described as significant had p values < 0.05 ($^{*}p < 0.05$, $^{**}p < 0.01$, $^{***}p < 0.001$). The nature of the interaction between AZD6244 and inhibitors of the MET-JAK1/2-STAT3 pathway was determined by calculating the CI according to the method of Chou and Talalay (1984).

SUPPLEMENTAL INFORMATION

Supplemental Information includes Supplemental Experimental Procedures, seven figures, and three tables and can be found with this article online at http://dx.doi.org/10.1016/j.celrep.2014.05.032.

AUTHOR CONTRIBUTIONS

S.V.S.: project development, experimental design, performance, evaluation, manuscript/figure preparation, review, and project coordination. M.K.: experimental design, performance, evaluation, and figure preparation. P.D.D.: experimental design, performance, evaluation, and figure preparation. R.C.: experimental design, performance, evaluation, and figure preparation. W.A.: bioinformatics. P.V.J.: bioinformatics. K.L.R.: experimental performance. T.S.: donation of isogenic *KRAS*WT/MT cell lines. S.S.: donation of isogenic *KRAS*WT/MT cell lines. J.B.: bioinformatics. P.M.: donation of c-MET constructs. C.F.: support of animal experiments. H.-J.L.: donation of tumor samples. M.L.: evaluation and manuscript review. D.B.L.: project development, experimental design, and manuscript review. P.G.J.: project development, experimental design, and manuscript review.

ACKNOWLEDGMENTS

This study was supported by Cancer Research UK (C212/A7402) and a Cancer Research UK fellowship (C13749/A13172). P.G.J. is employed by ALMAC Diagnostics and has ownership interest in both ALMAC Diagnostics and Fusion Antibodies. He is a consultant/advisor for, and has received honoraria from, Chugai Pharmaceuticals, Sanofi-Aventis, and Pfizer.

Received: August 24, 2012
Revised: March 1, 2014
Accepted: May 12, 2014
Published: June 12, 2014

REFERENCES

Allen, W.L., Stevenson, L., Coyle, V.M., Jithesh, P.V., Proutski, I., Carson, G., Gordon, M.A., Lenz, H.J., Van Schaeybroeck, S., Longley, D.B., and Johnston, P.G. (2012). A systems biology approach identifies SART1 as a novel determinant of both 5-fluorouracil and SN38 drug resistance in colorectal cancer. Mol. Cancer Ther. *11*, 119–131.

Athauda, G., Giubellino, A., Coleman, J.A., Horak, C., Steeg, P.S., Lee, M.J., Trepel, J., Wimberly, J., Sun, J., Coxon, A., et al. (2006). c-Met ectodomain shedding rate correlates with malignant potential. Clin. Cancer Res. *12*, 4154–4162.

Babij, C., Zhang, Y., Kurzeja, R.J., Munzli, A., Shehabeldin, A., Fernando, M., Quon, K., Kassner, P.D., Ruefli-Brasse, A.A., Watson, V.J., et al. (2011). STK33 kinase activity is nonessential in KRAS-dependent cancer cells. Cancer Res. *71*, 5818–5826.

Barbie, D.A., Tamayo, P., Boehm, J.S., Kim, S.Y., Moody, S.E., Dunn, I.F., Schinzel, A.C., Sandy, P., Meylan, E., Scholl, C., et al. (2009). Systematic RNA interference reveals that oncogenic KRAS-driven cancers require TBK1. Nature *462*, 108–112.

Biscardi, J.S., Maa, M.C., Tice, D.A., Cox, M.E., Leu, T.H., and Parsons, S.J. (1999). c-Src-mediated phosphorylation of the epidermal growth factor receptor on Tyr845 and Tyr1101 is associated with modulation of receptor function. J. Biol. Chem. *274*, 8335–8343.

Chang, J.T., Carvalho, C., Mori, S., Bild, A.H., Gatza, M.L., Wang, Q., Lucas, J.E., Potti, A., Febbo, P.G., West, M., and Nevins, J.R. (2009). A genomic strategy to elucidate modules of oncogenic pathway signaling networks. Mol. Cell *34*, 104–114.

Chou, T.C., and Talalay, P. (1984). Quantitative analysis of dose-effect relationships: the combined effects of multiple drugs or enzyme inhibitors. Adv. Enzyme Regul. *22*, 27–55.

Clark, R., Wong, G., Arnheim, N., Nitecki, D., and McCormick, F. (1985). Antibodies specific for amino acid 12 of the ras oncogene product inhibit GTP binding. Proc. Natl. Acad. Sci. USA *82*, 5280–5284.

Comoglio, P.M., Giordano, S., and Trusolino, L. (2008). Drug development of MET inhibitors: targeting oncogene addiction and expedience. Nat. Rev. Drug Discov. *7*, 504–516.

Corvinus, F.M., Orth, C., Moriggl, R., Tsareva, S.A., Wagner, S., Pfitzner, E.B., Baus, D., Kaufmann, R., Huber, L.A., Zatloukal, K., et al. (2005). Persistent STAT3 activation in colon cancer is associated with enhanced cell proliferation and tumor growth. Neoplasia *7*, 545–555.

Garcia, R., Bowman, T.L., Niu, G., Yu, H., Minton, S., Muro-Cacho, C.A., Cox, C.E., Falcone, R., Fairclough, R., Parsons, S., et al. (2001). Constitutive activation of Stat3 by the Src and JAK tyrosine kinases participates in growth regulation of human breast carcinoma cells. Oncogene *20*, 2499–2513.

Grivennikov, S., Karin, E., Terzic, J., Mucida, D., Yu, G.Y., Vallabhapurapu, S., Scheller, J., Rose-John, S., Cheroutre, H., Eckmann, L., and Karin, M. (2009).

IL-6 and Stat3 are required for survival of intestinal epithelial cells and development of colitis-associated cancer. Cancer Cell *15*, 103–113.

Hart, S., Fischer, O.M., Prenzel, N., Zwick-Wallasch, E., Schneider, M., Hennighausen, L., and Ullrich, A. (2005). GPCR-induced migration of breast carcinoma cells depends on both EGFR signal transactivation and EGFR-independent pathways. Biol. Chem. *386*, 845–855.

Hedvat, M., Huszar, D., Herrmann, A., Gozgit, J.M., Schroeder, A., Sheehy, A., Buettner, R., Proia, D., Kowolik, C.M., Xin, H., et al. (2009). The JAK2 inhibitor AZD1480 potently blocks Stat3 signaling and oncogenesis in solid tumors. Cancer Cell *16*, 487–497.

Jhawer, M., Goel, S., Wilson, A.J., Montagna, C., Ling, Y.H., Byun, D.S., Nasser, S., Arango, D., Shin, J., Klampfer, L., et al. (2008). PIK3CA mutation/PTEN expression status predicts response of colon cancer cells to the epidermal growth factor receptor inhibitor cetuximab. Cancer Res. *68*, 1953–1961.

Kong-Beltran, M., Stamos, J., and Wickramasinghe, D. (2004). The Sema domain of Met is necessary for receptor dimerization and activation. Cancer Cell *6*, 75–84.

Kyula, J.N., Van Schaeybroeck, S., Doherty, J., Fenning, C.S., Longley, D.B., and Johnston, P.G. (2010). Chemotherapy-induced activation of ADAM-17: a novel mechanism of drug resistance in colorectal cancer. Clin. Cancer Res. *16*, 3378–3389.

Lemjabbar-Alaoui, H., Sidhu, S.S., Mengistab, A., Gallup, M., and Basbaum, C. (2011). TACE/ADAM-17 phosphorylation by PKC-epsilon mediates premalignant changes in tobacco smoke-exposed lung cells. PLoS ONE *6*, e17489.

Little, A.S., Balmanno, K., Sale, M.J., Newman, S., Dry, J.R., Hampson, M., Edwards, P.A., Smith, P.D., and Cook, S.J. (2011). Amplification of the driving oncogene, KRAS or BRAF, underpins acquired resistance to MEK1/2 inhibitors in colorectal cancer cells. Sci. Signal. *4*, ra17.

Luo, J., Emanuele, M.J., Li, D., Creighton, C.J., Schlabach, M.R., Westbrook, T.F., Wong, K.K., and Elledge, S.J. (2009). A genome-wide RNAi screen identifies multiple synthetic lethal interactions with the Ras oncogene. Cell *137*, 835–848.

Maughan, T.S., Adams, R.A., Smith, C.G., Meade, A.M., Seymour, M.T., Wilson, R.H., Idziaszczyk, S., Harris, R., Fisher, D., Kenny, S.L., et al.; MRC COIN Trial Investigators. (2011). Addition of cetuximab to oxaliplatin-based first-line combination chemotherapy for treatment of advanced colorectal cancer: results of the randomised phase 3 MRC COIN trial. Lancet *377*, 2103–2114.

Merchant, N.B., Voskresensky, I., Rogers, C.M., Lafleur, B., Dempsey, P.J., Graves-Deal, R., Revetta, F., Foutch, A.C., Rothenberg, M.L., Washington, M.K., and Coffey, R.J. (2008). TACE/ADAM-17: a component of the epidermal growth factor receptor axis and a promising therapeutic target in colorectal cancer. Clin. Cancer Res. *14*, 1182–1191.

Michieli, P., Mazzone, M., Basilico, C., Cavassa, S., Sottile, A., Naldini, L., and Comoglio, P.M. (2004). Targeting the tumor and its microenvironment by a dual-function decoy Met receptor. Cancer Cell *6*, 61–73.

Mora, L.B., Buettner, R., Seigne, J., Diaz, J., Ahmad, N., Garcia, R., Bowman, T., Falcone, R., Fairclough, R., Cantor, A., et al. (2002). Constitutive activation of Stat3 in human prostate tumors and cell lines: direct inhibition of Stat3 signaling induces apoptosis of prostate cancer cells. Cancer Res. *62*, 6659–6666.

Morikawa, T., Baba, Y., Yamauchi, M., Kuchiba, A., Nosho, K., Shima, K., Tanaka, N., Huttenhower, C., Frank, D.A., Fuchs, C.S., and Ogino, S. (2011). STAT3 expression, molecular features, inflammation patterns, and prognosis in a database of 724 colorectal cancers. Clin. Cancer Res. *17*, 1452–1462.

Murphy, G. (2008). The ADAMs: signalling scissors in the tumour microenvironment. Nat. Rev. Cancer *8*, 929–941.

Nemunaitis, J., Cox, J., Hays, S., Meyer, W., Kebart, R., Ognoskie, N., Courtney, A., Yu, Y., Rasmussen, H., and Tong, A. (2000). Prognostic role of K-ras in patients with progressive colon cancer who received treatment with Marimastat (BB2516). Cancer Invest. *18*, 185–190.

Prahallad, A., Sun, C., Huang, S., Di Nicolantonio, F., Salazar, R., Zecchin, D., Beijersbergen, R.L., Bardelli, A., and Bernards, R. (2012). Unresponsiveness of colon cancer to BRAF(V600E) inhibition through feedback activation of EGFR. Nature *483*, 100–103.

Scholl, C., Fröhling, S., Dunn, I.F., Schinzel, A.C., Barbie, D.A., Kim, S.Y., Silver, S.J., Tamayo, P., Wadlow, R.C., Ramaswamy, S., et al. (2009). Synthetic lethal interaction between oncogenic KRAS dependency and STK33 suppression in human cancer cells. Cell *137*, 821–834.

Seals, D.F., and Courtneidge, S.A. (2003). The ADAMs family of metalloproteases: multidomain proteins with multiple functions. Genes Dev. *17*, 7–30.

Sen, B., Peng, S., Saigal, B., Williams, M.D., and Johnson, F.M. (2011). Distinct interactions between c-Src and c-Met in mediating resistance to c-Src inhibition in head and neck cancer. Clin. Cancer Res. *17*, 514–524.

Shirasawa, S., Furuse, M., Yokoyama, N., and Sasazuki, T. (1993). Altered growth of human colon cancer cell lines disrupted at activated Ki-ras. Science *260*, 85–88.

Stevenson, L., Allen, W.L., Turkington, R., Jithesh, P.V., Proutski, I., Stewart, G., Lenz, H.J., Van Schaeybroeck, S., Longley, D.B., and Johnston, P.G. (2012). Identification of galanin and its receptor GalR1 as novel determinants of resistance to chemotherapy and potential biomarkers in colorectal cancer. Clin. Cancer Res. *18*, 5412–5426.

Torrance, C.J., Agrawal, V., Vogelstein, B., and Kinzler, K.W. (2001). Use of isogenic human cancer cells for high-throughput screening and drug discovery. Nat. Biotechnol. *19*, 940–945.

Van Cutsem, E., Köhne, C.H., Láng, I., Folprecht, G., Nowacki, M.P., Cascinu, S., Shchepotin, I., Maurel, J., Cunningham, D., Tejpar, S., et al. (2011). Cetuximab plus irinotecan, fluorouracil, and leucovorin as first-line treatment for metastatic colorectal cancer: updated analysis of overall survival according to tumor KRAS and BRAF mutation status. J. Clin. Oncol. *29*, 2011–2019.

Van Schaeybroeck, S., Kelly, D.M., Kyula, J., Stokesberry, S., Fennell, D.A., Johnston, P.G., and Longley, D.B. (2008). Src and ADAM-17-mediated shedding of transforming growth factor-alpha is a mechanism of acute resistance to TRAIL. Cancer Res. *68*, 8312–8321.

Van Schaeybroeck, S., Kyula, J.N., Fenton, A., Fenning, C.S., Sasazuki, T., Shirasawa, S., Longley, D.B., and Johnston, P.G. (2011). Oncogenic Kras promotes chemotherapy-induced growth factor shedding via ADAM17. Cancer Res. *71*, 1071–1080.

Wernig, G., Kharas, M.G., Okabe, R., Moore, S.A., Leeman, D.S., Cullen, D.E., Gozo, M., McDowell, E.P., Levine, R.L., Doukas, J., et al. (2008). Efficacy of TG101348, a selective JAK2 inhibitor, in treatment of a murine model of JAK2V617F-induced polycythemia vera. Cancer Cell *13*, 311–320.

Zhou, B.B., Peyton, M., He, B., Liu, C., Girard, L., Caudler, E., Lo, Y., Baribaud, F., Mikami, I., Reguart, N., et al. (2006). Targeting ADAM-mediated ligand cleavage to inhibit HER3 and EGFR pathways in non-small cell lung cancer. Cancer Cell *10*, 39–50.